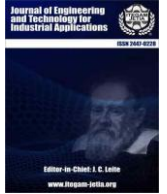




ISSN ONLINE: 2447-0228



## SUB-MODULE VOLTAGE ESTIMATION OF MODULAR MULTILEVEL CONVERTER IN PV APPLICATIONS USING A SLIDING MODE OBSERVER

Imane Alia <sup>1</sup>, Imad Merzouk <sup>2</sup> and Mehamed Mounir Rezaoui <sup>3</sup>

<sup>1</sup> ABC Institute – ABCI. Manaus-Amazonas, Brazil.

<sup>2,3</sup> Laboratory of Applied Automation and Industrial Diagnostics Laboratory (LAADI), Faculty of Sciences and Technology, University of Djelfa, PO Box 3117, Djelfa 17000.

<sup>1</sup><https://orcid.org/0009-0009-2516-8102>, <sup>2</sup><https://orcid.org/0000-0003-1539-1414>, <sup>3</sup><https://orcid.org/0000-0003-2761-6123>

Email: [alia.imane@univ-djelfa.dz](mailto:alia.imane@univ-djelfa.dz), [i.merzouk@univ-djelfa.dz](mailto:i.merzouk@univ-djelfa.dz), [mm\\_rezaoui@mail.univ-djelfa.dz](mailto:mm_rezaoui@mail.univ-djelfa.dz)

### ARTICLE INFO

#### Article History

Received: January 07, 2025

Revised: February 20, 2025

Accepted: March 15, 2025

Published: March 31, 2025

#### Keywords:

Modular Multilevel Converter, Sliding Mode Observer, Capacitor Voltage Estimation, Voltage Balancing Control, PV Application.

### ABSTRACT

This paper presents a Sliding Mode Observer (SMO) for estimating sub-module (SM) voltages in Modular Multilevel Converters (MMCs) used in photovoltaic (PV) applications. MMCs are widely favored in medium- and high-voltage applications due to their modularity and scalability. However, traditional voltage sensing methods require numerous sensors, increasing system complexity, cost, and susceptibility to sensor failures. The proposed SMO offers a robust alternative, providing accurate voltage estimation despite parameter variations and external disturbances. The design and implementation of the SMO, along with its integration into the MMC control strategy, are demonstrated. The observer performance is validated through simulations and Matlab results, which demonstrate effective voltage estimation across different operating conditions. This method improves SM capacitor voltage balancing, enhances the reliable operation of MMCs in PV applications, and lowers costs.



Copyright ©2025 by authors and Galileo Institute of Technology and Education of the Amazon (ITEGAM). This work is licensed under the Creative Commons Attribution International License (CC BY 4.0).

### I. INTRODUCTION

Modular Multilevel Converters (MMCs) are increasingly used in photovoltaic (PV) systems because of their modular structure and clear superiority over conventional converters [1-3]. MMCs are composed of several sub-modules (SMs) connected in series. These converters offer numerous notable advantages that are especially valuable in renewable energy applications. Each sub-module generally comprises a capacitor and power electronic switches that can be controlled to generate specific voltage levels [4-7].

One notable characteristic of MMCs is their ability to scale, enabling them to achieve higher voltage levels by increasing the number of SMs. Scalability is important for PV systems, as they frequently necessitate high voltage conversion ratios to provide efficient energy transfer. Moreover, the modularity of MMCs improves the reliability of the system and provides more flexibility in maintenance. It is possible to bypass or replace particular system modules without impacting the entire system, thus enhancing fault tolerance and adaptability [8], [9].

MMCs are highly efficient and produce high-quality output. They distribute voltage stress across multiple SMs, resulting in reduced switching losses and increased efficiency. The multilevel output waveforms they produce have low harmonic distortion, which is essential for meeting grid integration and power quality standards in PV systems [10], [11].

An essential element of MMC operation is the efficient control of SM capacitor voltages. This involves controlling the average voltage across the capacitors at the leg level and ensuring voltage balance within each arm. To achieve efficient regulation of the average voltage and balancing of capacitor voltages in an MMC, a combination of modulation techniques and control strategies are required [12], [13].

As with any grid-connected converters, the DC-link voltage of MMCs is typically regulated using PI controllers. For capacitor voltage balancing, one of the most effective methods is a sorting algorithm, which selectively inserts or bypasses SMs. Alternatively, balance correction can be achieved using a PI controller, often in combination with Phase-Shifted Carrier Pulse-Width Modulation (PSC-PWM) [13-15].

Sorting algorithm techniques rely on multiple separate sensors to measure individual SM voltages and arm currents. However, the use of extensive sensor networks increases system complexity and costs, posing significant challenges for practical implementation. Therefore, a key objective in the advancement of grid-connected MMC in PV systems is to reduce the total number of sensors while still ensuring efficient control [16]. To overcome these issues, sensorless capacitor voltage control schemes have been developed using arm current measurements and DC-link voltage to estimate capacitor voltages.

These methods aim to simplify the system architecture, reduce costs, and enhance reliability, particularly in handling SM faults in PV systems, where ensuring stable and efficient operation is crucial. In [17] a new SM voltage estimation scheme for MMCs was introduced, employing a Kalman filter approach. This method decreases complexity and cost by utilizing only two voltage sensors per MMC leg, rather than one for each SM. It demonstrates accurate tracking of SM voltages, robustness to parameter variations like arm inductance changes, and effectiveness across various operational scenarios through simulation and experimental validation. Nevertheless, the suggested approach has many drawbacks.

There is a lack of thorough investigation into the effects of estimation deviations and an absence of discussions on computational complexity and comparative studies with alternative approaches. The paper [18] presents a novel method for estimating SM voltages in MMCs without additional sensors, using discretized SM voltage dynamics and a Kalman filter observer. Validated through simulations and experiments, the method shows robust performance. However, there is a limited comparison with existing methods and a need for more comprehensive comparisons. Despite these issues, the study offers promising advancements in reducing sensor count while ensuring accurate SM voltage estimation.

The state observer proposed in the paper [19] aims to estimate capacitor voltages and circulating currents in MMCs without direct voltage and current sensors. It utilizes system models and available measurements to estimate unmeasured states, facilitating effective capacitor voltage balancing and circulating current suppression. This sensorless control approach is streamlined but relies heavily on accurate system modeling and quality measurements to avoid estimation errors. Additionally, the ability of the observer to adapt to dynamic changes in operating conditions is essential for maintaining robustness and stability, which the article does not fully address.

The reference [20] introduces a capacitor voltage balancing strategy for MMCs using the ADALINE (Adaptive Linear Neuron) algorithm to estimate sub-module voltages instead of directly measuring them. This approach reduces the need for multiple voltage sensors and simplifies the control system. Simulation results show that the ADALINE algorithm accurately tracks sub-module voltages and effectively balances them under both steady-state and dynamic conditions.

The novelty of this work lies in its application of the ADALINE algorithm to MMC control, offering a lower-cost and simplified implementation. However, the paper lacks experimental validation and does not address the robustness of the ADALINE algorithm to parameter variations and disturbances in practical scenarios.

In [21] a novel approach to control MMC was presented, particularly focusing on single-phase applications. The authors propose an innovative Interconnected Observer (IO) based Model Predictive Control (MPC) strategy aimed at estimating capacitor

voltages using circulating and load currents. This method enhances system robustness by accommodating parameter uncertainties, such as capacitance variations. The integration of IO with MPC provides stable and balanced voltage control while minimizing circulating current, as demonstrated through Matlab/Simulink simulations. However, the paper primarily addresses a theoretical model with simulation validation, and practical implementation details are sparse.

However, although the observer demonstrates theoretical effectiveness, the authors neglect to provide additional examination to evaluate its sensitivity to model uncertainties and parameter changes. Additionally, the performance of the observer was not assessed under varying operating conditions, such as load changes and grid failures.

Nevertheless, selecting an appropriate estimation/observation method is a significant challenge for capacitor voltage estimation in MMCs. Despite numerous advanced estimation strategies, SMOs remain employed in several recently published research papers. SMOs have gained special interest due to their rapid convergence rate, easy implementation, and low cost.

The paper [22] proposes a method to estimate individual capacitor voltages in an MMC using only arm current measurements and modulating signals, thereby eliminating the need for voltage sensors. The sliding-mode observer is validated through simulations under various conditions, demonstrating its robustness against external disturbances, parametric variations, and dynamics.

In [23] a method for controlling MMCs without using voltage sensors was introduced. It employs a SMO to estimate capacitor voltages and a Voltage Tracking Fuzzy Controller (VTFC) for maintaining voltage balance. While the approach reduces sensor dependency and enhances reliability, several areas need improvement. The complexity and computational demands of implementing SMO and VTFC in real-time are not discussed, nor is the sensitivity of the SMO to parameter changes like capacitance or resistance variations. Although there are certain limitations, the method shows possibilities for reducing hardware complexity and improving MMC reliability.

A discrete-time SMO for controlling capacitor voltage in MMCs proposed by [24]. This technique estimates capacitor voltages and arm currents without additional sensors, potentially lowering system costs and complexity.

This study presents the implementation of a SMO for the estimation of SM voltages in grid-connected MMCs used in PV systems. The suggested method aims to provide precise voltage estimations while minimizing the need for sensors, thus improving control performance and system resilience in grid-connected PV systems. The simulation findings confirm that the SMO has high dynamic, good stability, and robustness when subjected to variations in irradiance profile, switching frequency, and parameter changes.

The structure of this paper is as follows: Section II explains the general system configuration used in this research. Section III provides a detailed description of the estimation technique. Section IV discusses the proposed control system, focusing primarily on grid-connected PV systems. Section V presents the simulation results, and finally, Section VI concludes the paper.

## **II. OVERALL SYSTEM CONFIGURATION**

The configuration of an MMC-based single-phase grid-connected PV system is illustrated in Figure 1.

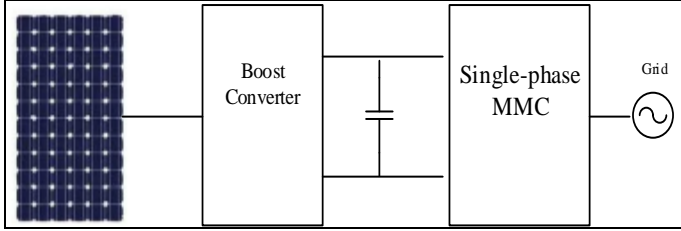


Figure 1: Grid-integrated PV system.  
Source: Authors, (2025).

This system consists of two main stages:

The first stage is a DC-DC boost converter, which extracts maximum power from the PV array using MPPT control. This converter steps up the PV voltage to a higher level, making it suitable for the second stage.

The second stage is a single-phase grid-connected MMC that converts the DC voltage from the boost converter into a sinusoidal AC voltage, synchronized with the grid.

### II.1 MMC STRUCTURE

A single-phase grid-connected MMC is shown in Figure 2. It consists of several key components. Each arm of the MMC (upper and lower) contains multiple SMs connected in series, with each SM typically comprising a half-bridge. The arms also include inductors. The boost provides the main DC voltage and connects the upper and lower arms. The converter connects to the AC grid through a filter.

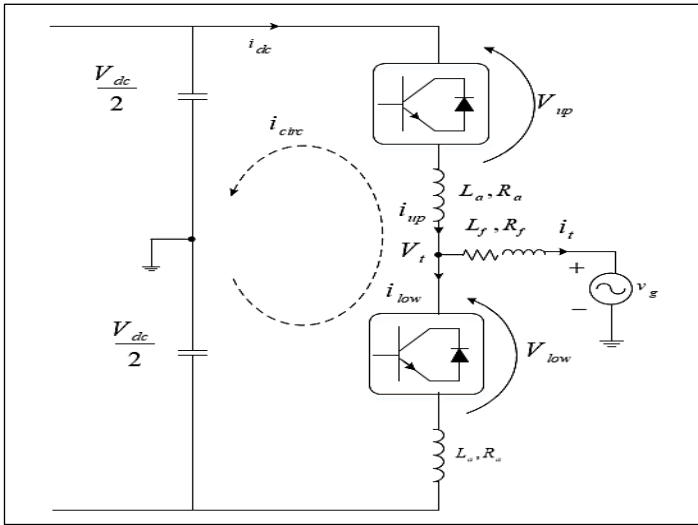


Figure 2: MMC topology.  
Source: Authors, (2025).

### II.2 MODELING OF THE MMC

The following equations model the system shown in Figure 2 [25], [26]:

$$\begin{cases} \frac{V_{dc}}{2} - L_a \frac{di_{up}}{dt} - R_a i_{up} - V_{up} = V_t \\ -\frac{V_{dc}}{2} + L_a \frac{di_{low}}{dt} + R_a i_{low} + V_{low} = V_t \end{cases} \quad (1), (2)$$

Because of the symmetrical structure of the MMC, it is assumed that AC output current ( $i_t$ ) is uniformly divided between the upper and lower arms of leg:

$$i_t = i_{up} - i_{low} \quad (3)$$

Arm currents in a MMC comprise both  $i_t$  and DC current, also known as the circulating current ( $i_{circ}$ ). The relations between  $i_t$ ,  $i_{up}$ ,  $i_{low}$ , and  $i_{circ}$  are defined:

$$\begin{cases} i_{up} = \frac{i_t}{2} + i_{circ} \\ i_{low} = -\frac{i_t}{2} + i_{circ} \end{cases} \quad (4)$$

The  $i_t$  represents the primary current that passes through the converter and is directed to the grid. It is the fundamental current that the converter is designed to generate and regulate. The  $i_{circ}$  within the converter does not directly contribute to the  $i_t$ . It traverses through both the two arms, and its expression can be stated as follows:

$$i_{circ} = \frac{i_{up} + i_{low}}{2} \quad (5)$$

A based the fundamental equations of the system:

1)The  $i_{circ}$  can be determined as follows: by summing the two Equations (1), (2), and replace  $i_{circ}$  by Equation (5):

$$L_a \frac{di_{circ}}{dt} + R_a i_{circ} = \frac{V_{dc} - (V_{up} + V_{low})}{2} \quad (6)$$

The  $i_{circ}$  is determined by the difference between the  $V_{dc}$  and the sum of the  $V_{up}$  and  $V_{low}$ .

$$v_{circ} = L_a \frac{di_{circ}}{dt} + R_a i_{circ} \quad (7)$$

$v_{circ}$ : The voltage caused by  $i_{circ}$ .

2)And in the case of subtracting Equations (1), (2), and replace for Equation (3) obtain:

$$V_t = \frac{V_{low} - V_{up}}{2} + \frac{L_a}{2} \frac{di_t}{dt} + R_a i_t \quad (8)$$

The  $\frac{V_{low} - V_{up}}{2}$  this term is the inner EMF (electromotive force) of phase, and defined by:

$$V_t^* = \frac{V_{low} - V_{up}}{2} \quad (9)$$

$i_t$  is given:

$$L_f \frac{di_t}{dt} + R_f i_t = v_g - V_t \quad (10)$$

Equations (8) and (9) combined could produce the MMC dynamics:

$$V_t = V_t^* + \left( \frac{L_a}{2} + L_f \right) \frac{di_t}{dt} + \left( \frac{R_a}{2} + R_f \right) i_t \quad (11)$$

$R_s$  and  $L_s$  are given as follows:

$$\begin{aligned} L_s &= \frac{L_a}{2} + L_f \\ R_s &= \frac{R_a}{2} + R_f \end{aligned} \quad (12)$$

The voltage reference for controlling the upper and lower SMs of the MMC is defined by Equation (13):

$$\begin{cases} V_{up} = \frac{V_{dc}}{2} - V_t^* - v_{circ} \\ V_{low} = \frac{V_{dc}}{2} + V_t^* - v_{circ} \end{cases} \quad (13)$$

### III. PROPOSED SM VOLTAGE ESTIMATION SCHEME

The Sliding Mode Observer (SMO) is a well-known algorithm extensively used in various fields. It is robust to parameter fluctuations and external disturbances and has precise finite-time convergence characteristics [27], [28].

In this section, the Sliding Mode Observer (SMO) is designed, and the stability analysis of the observer is provided. The SMO uses the arm currents and DC-link voltage to estimate the capacitor voltages. A voltage-sensorless operation utilizing the SMO is developed to replace voltage measurements, as indicated in the following equations [23]:

This paper focuses on the upper arm as an example. The voltage of the upper arm can be represented as follows, noting that  $i$  refers to the  $i$ -th SM ( $i = 1, 2, \dots, 2N$ ):

$$V_{ci} = \frac{1}{C} \int_0^t S_i(t) i_{up}(t) dt + V_{ci}(0) \quad (14)$$

For SMO, the state variables are chosen to be the voltage across the capacitor and the current through the arm. The continuous-time sliding mode function allows for the acquisition of the voltage across the upper arm capacitor and the current flowing through the arm:

$$\begin{aligned} \frac{d\hat{V}_{ci}}{dt} &= \frac{1}{C} S_i \hat{i}_{up} + \\ &k_{uf} \left( \sum_{i=1}^N S_i V_{ci} - \sum_{i=1}^N S_i \hat{V}_{ci} \right) \end{aligned} \quad (15)$$

$$\begin{aligned} \frac{d\hat{i}_{up}}{dt} &= \frac{1}{L_a} \left[ \frac{V_{dc}}{2} - \sum_{i=1}^N S_i \hat{V}_{ci} - R_a \hat{i}_{up} - V_t \right] + \\ &k_{if} \left( \sum_{i=1}^N i_{up} - \sum_{i=1}^N \hat{i}_{up} \right) \end{aligned} \quad (16)$$

A sign function, denoted as  $f(x)$ , is employed:

$$f(x) = \begin{cases} 1, & x > 0 \\ 0, & x = 0 \\ -1, & x < 0 \end{cases} \quad (17)$$

$$\frac{d\dot{V}_{ci}}{dt} = \frac{1}{C} S_i \dot{i}_{up} - k_{uf} \left( \sum_{i=1}^N S_i \dot{V}_{ci} \right) \quad (18)$$

$$\frac{d\dot{i}_{up}}{dt} = \frac{1}{L_a} \left( \sum_{i=1}^N S_i \dot{V}_{ci} \right) - k_{if} \dot{i}_{up} \quad (19)$$

Hence, the sliding surfaces are:

$$\sum_{i=1}^N S_i \dot{V}_{ci} = \left( \sum_{i=1}^N S_i V_{ci} - \sum_{i=1}^N S_i \hat{V}_{ci} \right) \quad (20)$$

$$\dot{i}_{up} = \left( i_{up} - \hat{i}_{up} \right) \quad (21)$$

Consequently, an equation for a Lyapunov candidate can be formulated:

$$V_e = \frac{1}{2} \left( \dot{i}_{up}^2 + \sum_{i=1}^N S_i \dot{V}_{ci}^2 \right) \quad (22)$$

$$\dot{V}_e^g = \frac{1}{2} \left( \dot{i}_{up} \ddot{i}_{up} + \sum_{i=1}^N S_i \dot{V}_{ci} \ddot{V}_{ci} \right) \quad (23)$$

$$\begin{aligned} \dot{V}_e^g &= \left\{ \frac{1}{L_a} \left( \sum_{i=1}^N S_i \dot{V}_{ci} \right) \dot{i}_{up} + k_{if} \left( \dot{i}_{up} \right) \right\} + \\ &\sum_{i=1}^N S_i \left\{ \frac{1}{C} S_i \dot{i}_{up} \dot{V}_{ci} - k_{uf} \left( \sum_{i=1}^N S_i \dot{V}_{ci} \right) \right\} \end{aligned} \quad (24)$$

To ensure  $V_e^g \leq 0$  adapts to all conditions, the following inequalities must be met.

$$\frac{1}{L_a} \left( \sum_{i=1}^N S_i \dot{V}_{ci} \right) \dot{i}_{up} \leq k_i$$

$$\frac{1}{C} S_i \dot{i}_{up} \dot{V}_{ci} \leq k_u \quad (25)$$

#### IV. CONTROL SYSTEM FOR THE MMC

The objective of this part is to design a novel controller for a single-phase grid-connected MMC-based PV system, with the goal of achieving comprehensive control over the system.

Figure 3 presents a detailed control scheme for the considered system. Before delving into the explanation of system control in this section, it is essential to highlight that the primary objective of this paper is not to address the issue of DC-DC converter control. However, it is important to note that the technique used for MPPT is Incremental Conductance (IC).

Thus, the regulator for MMC will be designed by combining 2 primary phases [29]:

- Output power control.
- Internal dynamics control of the MMC.

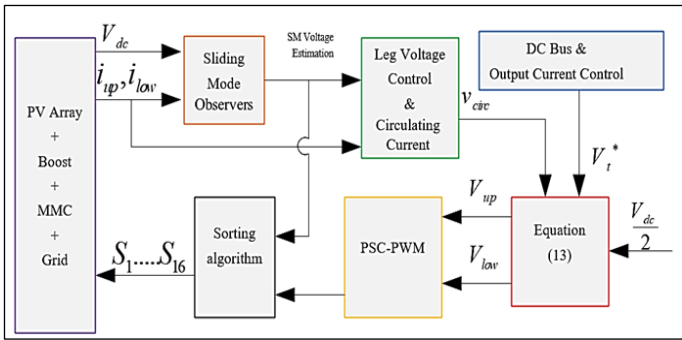


Figure 3: Overall control diagram. Source: Authors, (2025).

#### IV.1 OUTPUT POWER CONTROL

The design of the output power control for a grid-connected PV system involves three control loops:

##### IV.1.1 INNER CONTROL LOOP: GRID CURRENT CONTROL

The inner control loop is developed using a Proportional-Resonant (PR) controller. This loop directly acts on the grid current, ensuring precise regulation and stability of the current injected into the grid.

##### IV.1.2 OUTER CONTROL LOOP: CONTROL OF THE DC BUS

A Proportional-Integral (PI) controller is used in the outer control loop to maintain the DC bus voltage at a reference level. The reference of this controller is derived from the output active power.

##### IV.1.3 PHASE-LOCKED LOOP: GRID SYNCHRONIZATION

Grid synchronization is achieved using a Phase-Locked Loop (PLL), which determines the reference current angle. The PLL ensures that the inverter output is in phase with the grid voltage, facilitating proper synchronization and seamless operation.

These three control loops work together to achieve the desired control performance of the output power.

#### IV.2 INTERNAL DYNAMICS CONTROL OF THE MMC

The main aspects of internal dynamics control in MMCs are:

##### IV.2.1 CONTROL OF AVERAGE SM VOLTAGE BALANCING AND CIRCULATING CURRENT

The control loop is designed based on the reference [30]. The Average SM Voltage Balancing Control uses a Proportional-Integral (PI) controller to maintain the average voltage of the SM at a specified level that aligns with the SM capacitor voltage. The PI controller takes input from the average values of the SM capacitor voltages, calculated by dividing the total estimated capacitor voltages (obtained from the SMO) by the number of SMs in the leg (2N). The output of the PI controller adjusts the reference value for the circulating current. A Proportional-Resonant (PR) controller is used for circulating current control [31], [32].

##### IV.2.2 CONTROL OF INDIVIDUAL SM VOLTAGE BALANCING

Individual SM voltage balancing control typically involves a sorting algorithm, which selects the appropriate SMs to be inserted or bypassed based on the direction of the arm currents. This process ensures that the capacitor voltages are balanced, maintaining safe operating limits for the MMC [14].

The voltage commands produced by the two PR controllers, which control the grid current and circulating current, are utilized for the generation of SM voltage references.

#### IV.3 MODULATION TECHNIQUE

PSC-PWM is a widely used modulation strategy for multilevel inverters that employs phase-shifted carrier signals to synthesize the output voltage waveform with reduced harmonics [33], [34]. PSC-PWM generates the switching signals for the power devices. PSC-PWM takes the voltage references for each SM and produces the corresponding switching states to control the power devices within each SM. This integration allows the MMC to synthesize the desired output voltage waveform by accurately managing the switching of the individual SMs.

#### V. SIMULATION ANALYSES

To verify the effectiveness of the control strategy proposed in this paper, simulations were conducted using Matlab/Simulink software. The control system utilizes a SMO to estimate the capacitor voltages of the MMC. This approach was simulated and compared to a sensor-based method. Evaluations included responses under stable operating conditions, dynamic responses to variations in irradiance and switching frequency, and robustness against changes in capacitor values. The parameters of the grid-connected MMC are listed: P =3kW,  $v_g =230V$ ,  $v_{dc} =800 V$ , N=4,  $f_c = 4kHz$ ,  $L_a =1mH$ ,  $R_a =0.1\Omega$ ,  $C=800\mu F$ ,  $L_f =8.4mH$ ,  $R_f =1\Omega$ .

### V.1 STEADY-STATE

In this part of the simulation results, the steady-state performance of the system under normal weather conditions is analyzed for both the sensor-based scheme and the proposed estimation scheme.

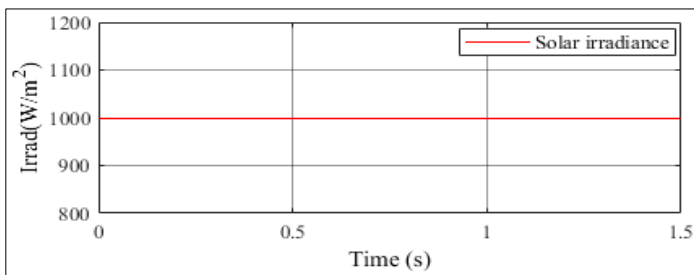
Case 1: In the sensor-based scheme, sensors are used to measure the following: (1) DC-link voltage, (2) grid voltages, (3) grid current, (4) arm currents, and (5) sub-module (SM) capacitor voltages (2N voltage sensors, where N is the number of SMs in each arm), as well as the PV output current and voltage. The simulation results are displayed in Figures 5.

Case 2: In the proposed estimation scheme, a Sliding Mode Observer (SMO) is used to estimate the capacitor voltages, with the simulation results displayed in Figures 6.

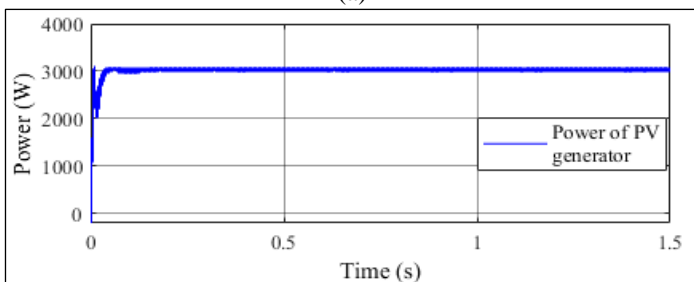
The results of the simulation shown in Figure 4 demonstrate that the MPPT technique performs well, delivering optimum power from the PV array to the grid with excellent performance characteristics under normal weather conditions.

In both schemes, whether it is a Case 1 or Case 2 scheme, the voltage loop controller of the internal dynamics control system effectively regulates the equilibrium of the sub-module capacitors, thereby eliminating circulating currents within the MMC. Consequently, the DC-link voltage is successfully maintained at its nominal value of 800 V. Additionally, the MMC is capable of generating a multilevel output voltage, which helps reduce harmonics and improve the overall power quality of the system. In both cases, the system provides a sinusoidal current with low ripple, closely synchronized with the grid voltage, thereby improving overall power quality. This demonstrates the effectiveness of the proposed observer, as it successfully maintains grid power quality in accordance with power quality standards.

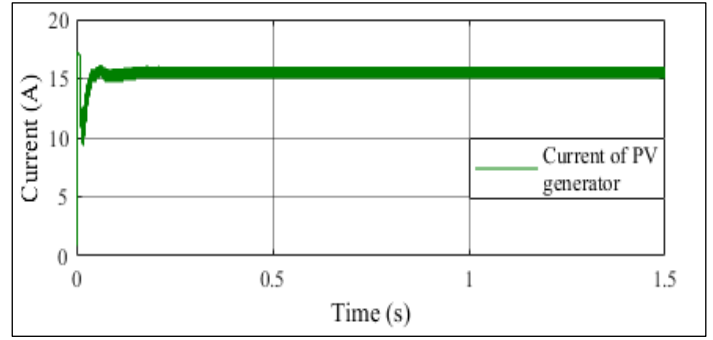
In general, the results demonstrate that both cases exhibit good and satisfactory performance in efficiently transferring energy from photovoltaic sources to the grid. However, the second case is particularly noteworthy for significantly reducing the number of sensors required, specifically by eliminating the eight sensors responsible for measuring capacitor voltages. This enhances control performance, lowers system costs, and increases reliability in grid-connected MMC systems. Reducing the number of sensors simplifies the control system, allowing it to focus on crucial parameters, which improves response times and stability.



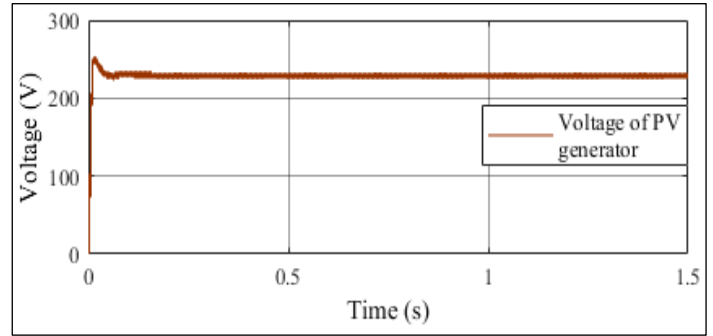
(a)



(b)



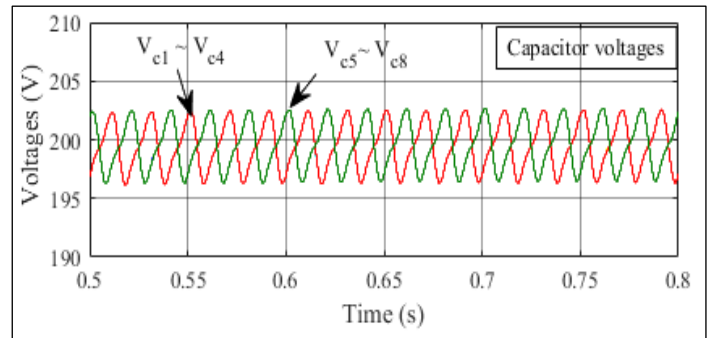
(c)



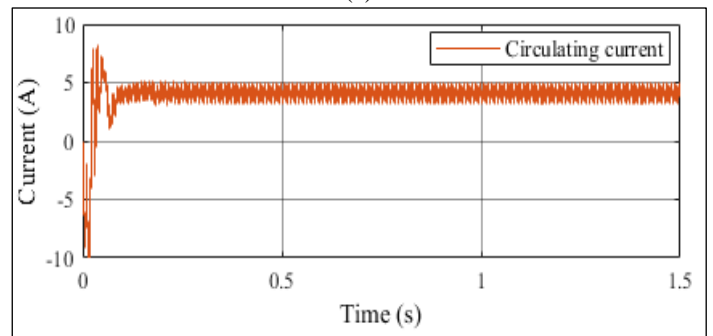
(d)

Figure 4: PV side results: (a) Irradiance profile, (b) PV output power, (c) PV output current, (d) PV output voltage.

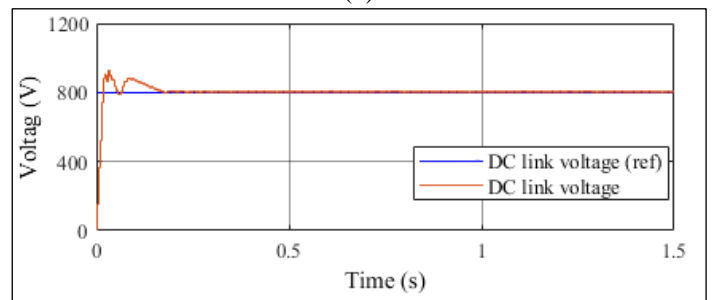
Source: Authors, (2025).



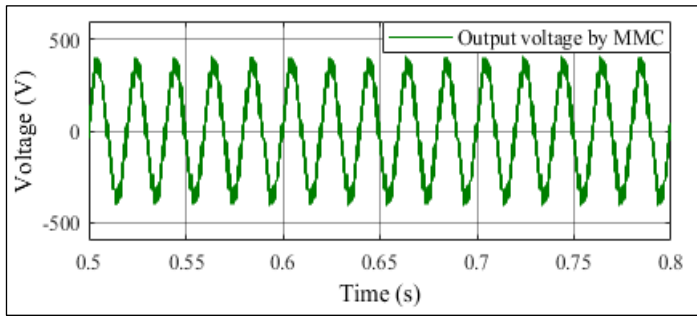
(a)



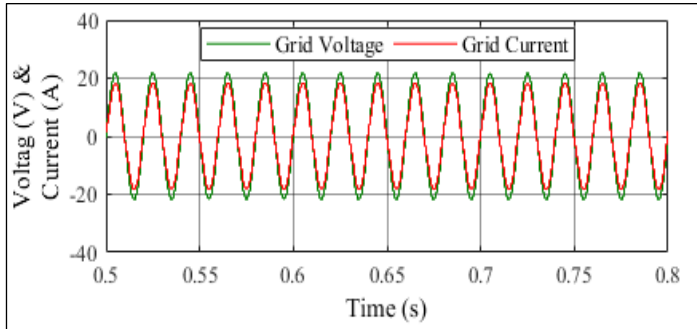
(b)



(c)

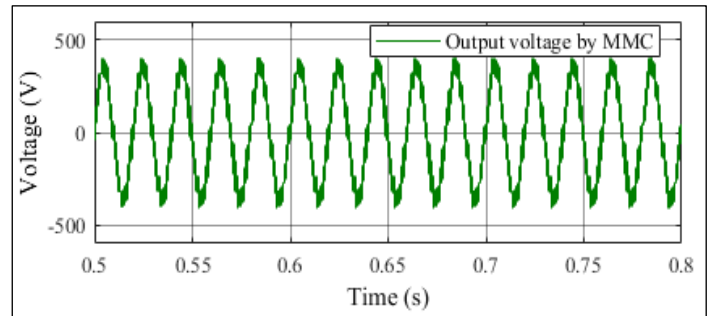


(d)

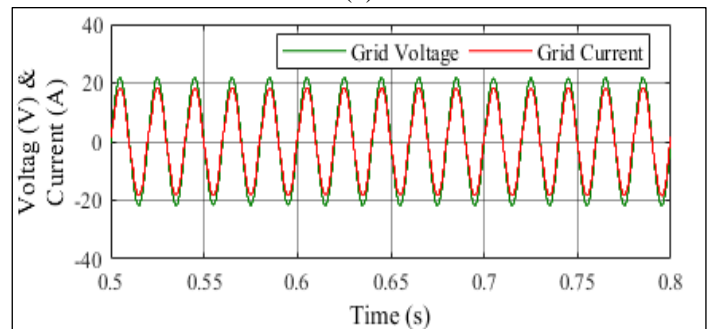


(e)

Figure 5: Case1 simulation results: (a) Capacitor voltages;(b) Circulating current error;(c)DC-link voltage;(d)Output voltage by MMC; (e).Grid phase voltage and current. Source: Authors, (2025).



(d)



(e)

Figure 6: Case2 simulation results:(a) Capacitor voltages, (b) Circulating current error, (c) DC-link voltage, (d) Output voltage by MMC, (e). Grid phase voltage and current. Source: Authors, (2025).

## V.2 DYNAMIC TEST

The dynamic test in the simulation results for the proposed estimation scheme involves analyzing the performance of the SMO under varying environmental conditions. This includes studying the impact of changes in solar irradiance and switching frequency. The simulations aim to model the dynamic behavior of the SMO for voltage sensor-less control of grid-connected MMCs, which is essential for understanding how the system responds to rapid fluctuations in such conditions.

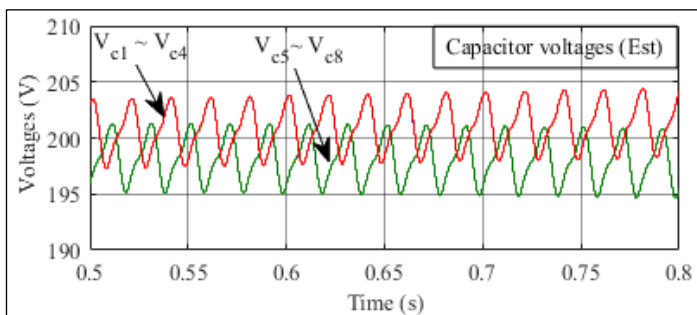
### V.2.1 CHANGES IN IRRADIANCE PROFILE

Figures (7-8) below illustrate the simulation results under various weather conditions, according to the irradiance profile shown in Figure 7a. As shown in Figure 7b, there is a direct correlation between variations in weather conditions and PV power

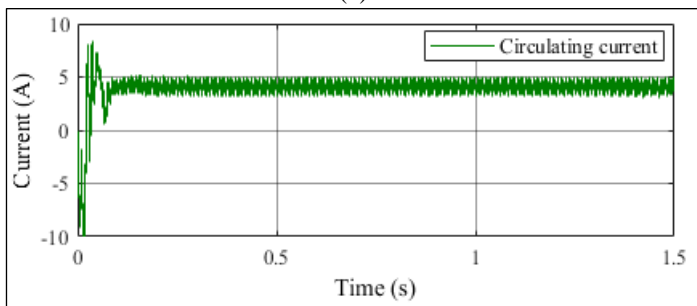
Figure 8.a displays the voltage levels of the upper and lower capacitors as estimated by the SMO. The results underscore that the MMC voltages remain maintained at their directed values. Accurate voltage estimation is essential for optimizing capacitor voltage balance, which significantly impacts the overall performance of the MMC.

The proposed algorithm provides good accuracy in estimating SM voltage. This is evident from the following results. Figure 8b indicates that a constant voltage above the reference value of 800V was maintained. The DC-link voltage is calculated by summing the SM voltages. In addition, Figure 8c demonstrates a direct proportionality between changes in irradiance and output current, indicating a corresponding change in output power.

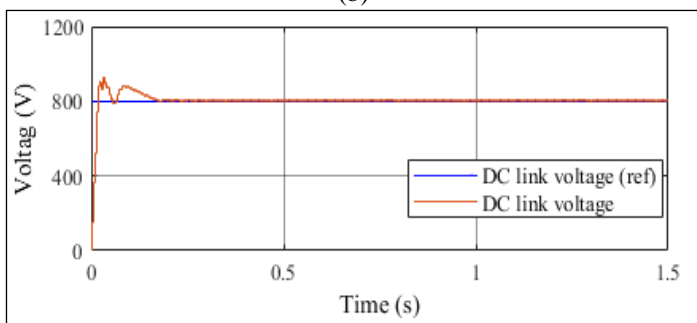
Figure 8d shows that the amplitudes of the circulating current and the capacitor voltage ripples are directly proportional to the active power, demonstrating the robust and reliable stability of the voltage estimation system.



(a)



(b)



(c)

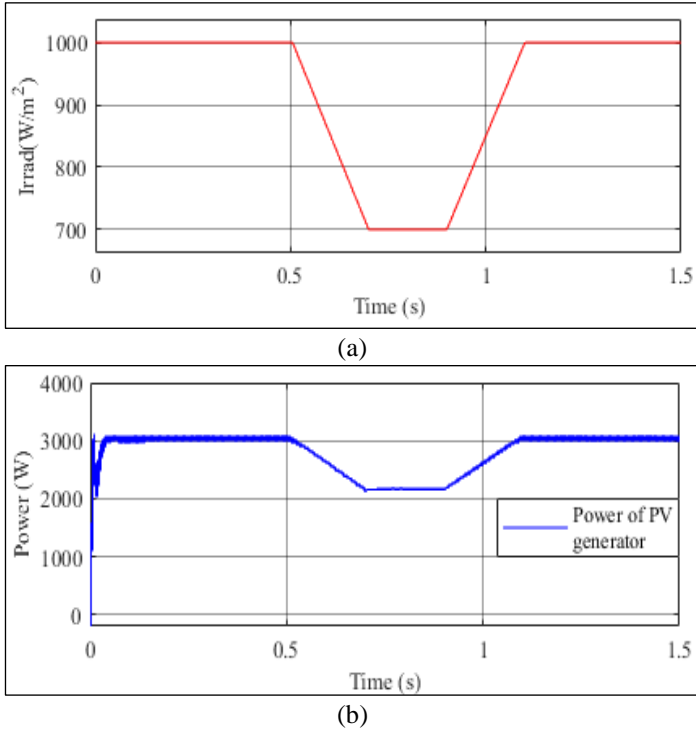


Figure 7: PV side results: (a) Irradiance profile (b), PV output power.

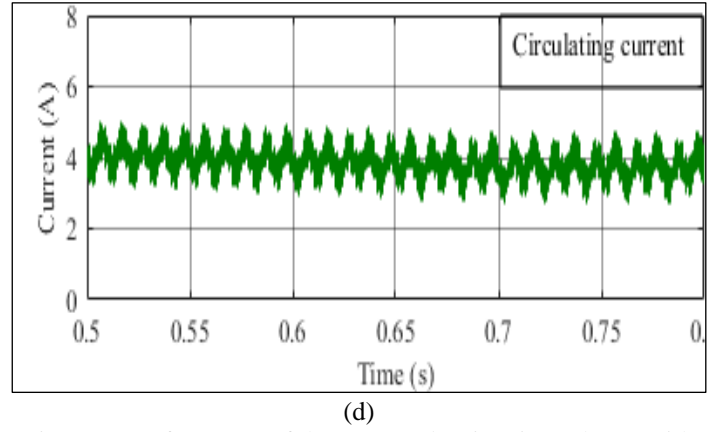
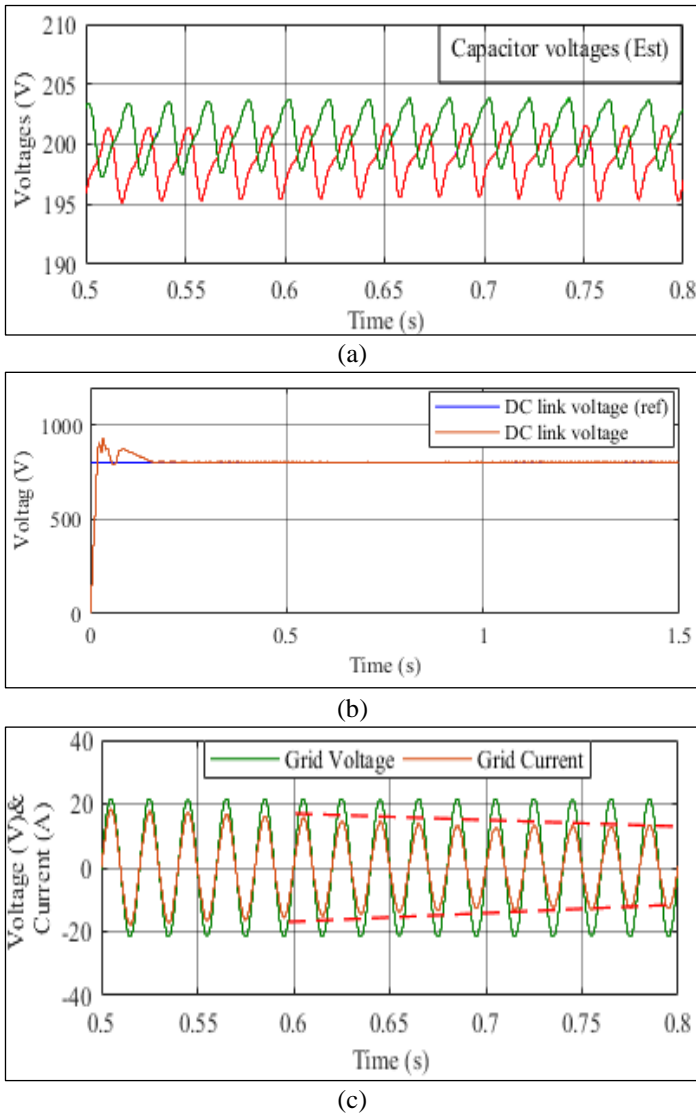
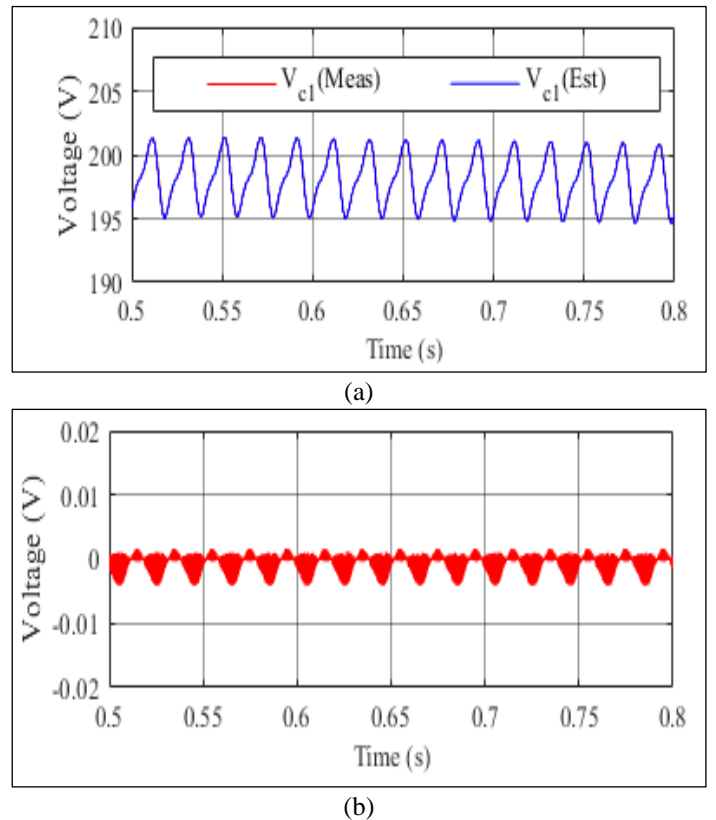


Figure 8: Performance of the proposed estimation scheme with changes in irradiance: (a) Estimated Capacitor voltages by SMO, (b) DC-link voltage, (c) Grid phase voltage and current, (d) Circulating current error .  
Source: Authors, (2025).

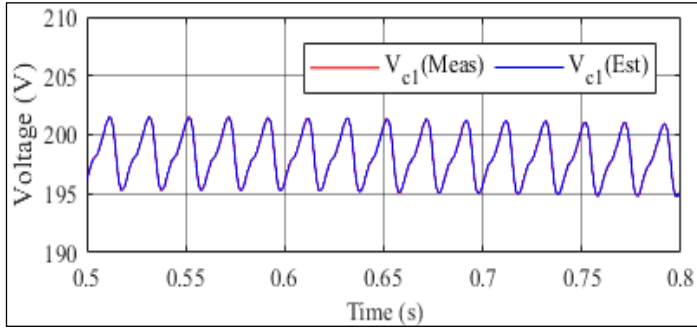
### V.2.2 CHANGES IN SWITCHING FREQUENCY

Figure 9 presents various switching frequencies to observe system dynamics and evaluate the effectiveness of the suggested controller. Despite the significant impact of switching frequency on capacitor voltage ripple and switching losses, the stability of capacitor voltage estimation, particularly for  $C_1$ , remains notable. The SMO demonstrates strong robustness, showing no observer error across cases, ensuring reliable voltage estimates despite frequency variations. While lower frequencies affect system dynamics and electrical parameters, their direct influence on output voltage and power transfer is important but beyond the scope of this study. This research emphasizes evaluating controller stability and performance under varying frequencies.

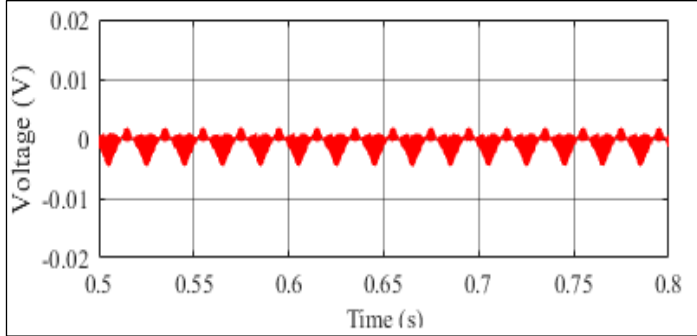


$f_c = 4 \text{ kHz}$



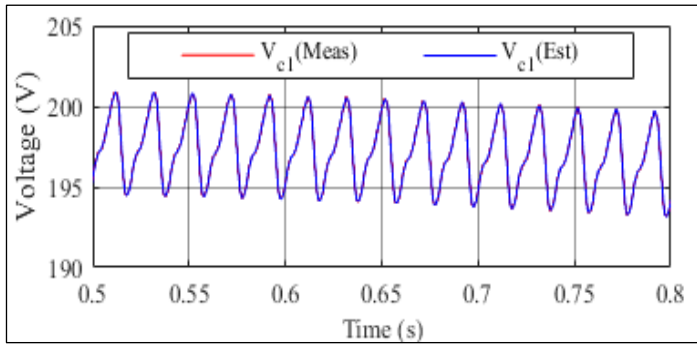


(a)

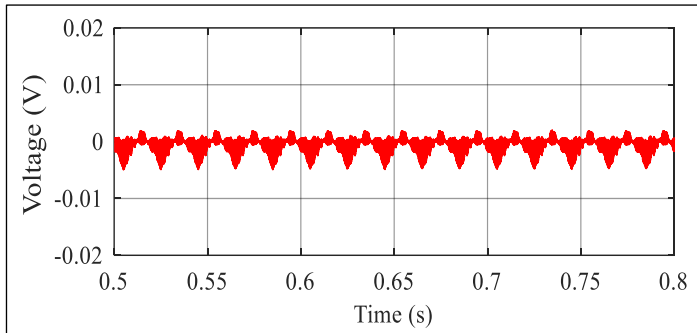


(b)

$f_c = 2 \text{ kHz}$



(a)



(b)

$f_c = 750 \text{ Hz}$

Figure 9: Performance of the proposed estimation scheme with changes in switching frequency for all eight SMs.

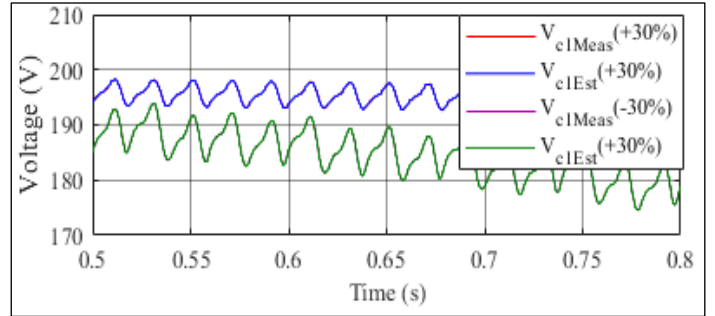
Source: Authors, (2025).

### V.2.3 ROBUSTNESS TEST

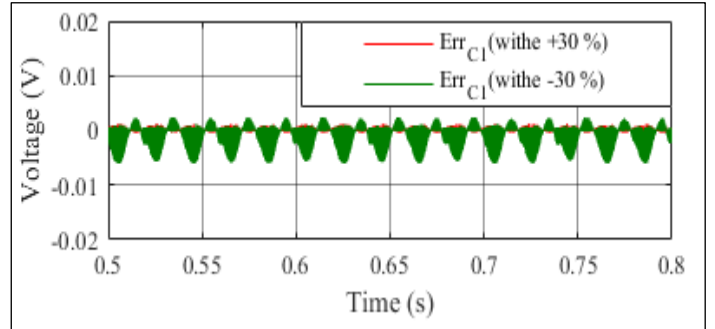
The robustness of the SMO is examined through variations in the capacitance values.

The reliability of the proposed algorithm for estimating SM voltage fluctuations in  $C_{j1}$  is confirmed by comparing the estimated SM capacitor voltage fluctuation with the measured value of when the nominal capacitance of the capacitor is increased or decreased

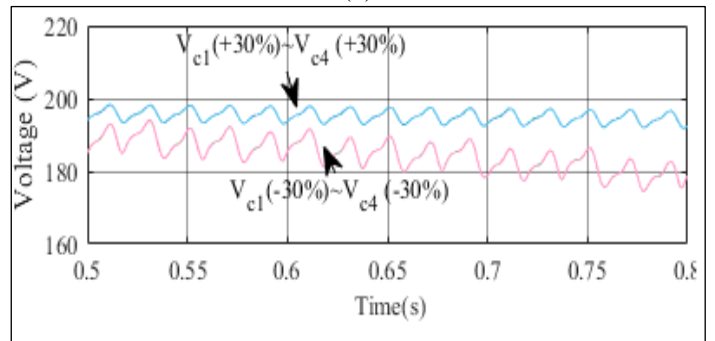
by 30%. This comparison is illustrated in Figure 10a. It is evident that the estimated SM voltage closely tracked the measured value of the individual SM voltages in terms of both shape and with nearly no observer errors, as shown in Figure 10b. The simulation results, which examined the SM voltage variations across the four SMs in the upper arm (Fig. 10c), showed that the SM capacitor voltages were maintained at a balanced level of 200 V (the nominal value limits). This ensured that the voltage fluctuations remained within the acceptable range specified by the system requirements. The proposed algorithm demonstrated high efficiency in estimating SM voltage variations.



(a)



(b)



(c)

Figure 10: Performance of the proposed estimation scheme with variations in all capacitors.

Source: Authors, (2025).

## VI. CONCLUSIONS

This study presented the development and application of a Sliding Mode Observer (SMO) for sub-module voltage estimation in Modular Multilevel Converters (MMCs) used in photovoltaic (PV) applications. The results demonstrate that the SMO provides a robust and reliable alternative to traditional voltage sensing methods, which are often cost-prohibitive and prone to sensor failures. By accurately estimating sub-module voltages without extensive physical sensors, the SMO enhances system reliability, reduces costs, and simplifies the hardware structure.

Simulation validations confirmed the effectiveness of the SMO in maintaining accurate voltage estimations both in steady-state and during dynamic changes. This improved voltage balancing and overall control of the MMC contributes to the safe and efficient operation of PV systems. Results from the studies show that the proposed method outperforms the sensor-based scheme.

In conclusion, the Sliding Mode Observer is a viable and effective solution for sub-module voltage estimation in MMCs. Its ability to mitigate the drawbacks of traditional voltage sensing methods positions it as a valuable tool for enhancing the performance and reliability of MMCs in PV applications. Future work should explore further optimization of the SMO design and its potential integration into other power electronic systems to fully leverage its benefits. Additionally, plan to implement it in an experimental environment in the future.

## VI. AUTHOR'S CONTRIBUTION

**Conceptualization:** Imane Alia, Imad Merzouk and Mehamed Mounir Rezaoui.

**Methodology:** Imane Alia, Imad Merzouk and Mehamed Mounir Rezaoui.

**Investigation:** Imane Alia, Imad Merzouk and Mehamed Mounir Rezaoui.

**Discussion of results:** Imane Alia, Imad Merzouk and Mehamed Mounir Rezaoui.

**Writing – Original Draft:** Imane Alia, Imad Merzouk and Mehamed Mounir Rezaoui.

**Writing – Review and Editing:** Imane Alia, Imad Merzouk and Mehamed Mounir Rezaoui.

**Resources:** Imane Alia, Imad Merzouk and Mehamed Mounir Rezaoui.

**Supervision:** Imane Alia, Imad Merzouk and Mehamed Mounir Rezaoui.

**Approval of the final text:** Imane Alia, Imad Merzouk and Mehamed Mounir Rezaoui.

## VII. REFERENCES

[1]Alotaibi, S., & Darwish, A. "Modular Multilevel Converters for Large-Scale Grid-Connected Photovoltaic Systems", A Review. *Energies*, 14(19), 6213, 2021. <https://doi.org/10.3390/en14196213>.

[2]Pu, H., Bai, Z., Xin, Y., Zhao, J., Bai, R., Luo, J., & Yi, J, "Efficient (2N+1) selective harmonic elimination in modular multilevel converters using an evolutionary many-tasking approach with prior knowledge", *Applied Soft Computing*, 144, 110468, 2023. <https://doi.org/10.1016/j.asoc.2023.110468>.

[3]Alia, I., Merzouk, I., & Rezaoui, M. M, "Robust line voltage sensor-less control of grid-connected MMC converter in PV Applications", *STUDIES IN ENGINEERING AND EXACT SCIENCES*, 5(1), 2366–2390, 2024. <https://doi.org/10.54021/seesv5n1-117>.

[4]Tian, Y., Wickramasinghe, H. R., Li, Z., Pou, J., & Konstantinou, G, "Review, Classification and Loss Comparison of Modular Multilevel Converter Submodules for HVDC Applications", *Energies*, 15(6), 1985, 2022. <https://doi.org/10.3390/en15061985>.

[5]An, Y., Sun, X., Ren, B., Li, H., & Zhang, M, "A data-driven method for IGBT open-circuit fault diagnosis for the modular multilevel converter based on a modified Elman neural network", *Energy Reports*, 8, 80–88, 2022. <https://doi.org/10.1016/j.egyr.2022.08.024>.

[6]Ke, L., Zhang, Y., Yang, B., Luo, Z., & Liu, Z, "Fault diagnosis with synchrosqueezing transform and optimized deep convolutional neural network: An application in modular multilevel converters", *Neurocomputing*, 430, 24–33,2021. <https://doi.org/10.1016/j.neucom.2020.11.037>.

[7]Barros, L. A. M., Martins, A. P., & Pinto, J. G, "A Comprehensive Review on Modular Multilevel Converters, Submodule Topologies, and Modulation Techniques", *Energies*, 15(3), 1078,2022. <https://doi.org/10.3390/en15031078>.

[8]Luo, Y., Jia, Z., Xu, L., Li, Q., & Song, Y, "A reduced switching frequency capacitor voltage balancing control for modular multilevel converters", *International Journal of Electrical Power & Energy Systems*, 2022. 142, 108272. <https://doi.org/10.1016/j.ijepes.2022.108272>.

[9]Ramirez, D., Zarei, M. E., Gupta, M., & Serrano, J, "Fast Model-based Predictive Control (FMPC) for grid connected Modular Multilevel Converters (MMC) ", *International Journal of Electrical Power & Energy Systems*, 119, 105951, . 2020. <https://doi.org/10.1016/j.ijepes.2020.105951>.

[10]Parvari, R., Filizadeh, S., & Muthumuni, D, "An accelerated detailed equivalent model for modular multilevel converters", *Electric Power Systems Research*, 223, 109648,2023. <https://doi.org/10.1016/j.epr.2023.109648>.

[11]Zhang, Y., Hu, H., Liu, Z., Zhao, M., & Cheng, L, "Concurrent fault diagnosis of modular multilevel converter with Kalman filter and optimized support vector machine", *Systems Science & Control Engineering*, 7(3), 43–53,2019. <https://doi.org/10.1080/21642583.2019.165084>.

[12]Li, Q., Li, B., He, J., Prieto-Araujo, E., Westerman Spier, D., Lyu, H., & Gomis-Bellmunt, O, "A novel design of circulating current control target to minimize SM capacitance in MMC", *International Journal of Electrical Power & Energy Systems*, 143, 108432, 2022. <https://doi.org/10.1016/j.ijepes.2022.108432>.

[13]Hu, P., Teodorescu, R., & Guerrero, J. M, "State observer based capacitor-voltage-balancing method for modular multilevel converters without arm-current sensors", *International Journal of Electrical Power & Energy Systems*, 113, 188–196, 2019. <https://doi.org/10.1016/j.ijepes.2019.05.025>.

[14]Zhao, J., Gu, C., Wu, S., Liu, W., Lei, Y., Hang, J., & Ding, S, "Improved power loss balance control for modular multilevel converters based on variable capacitor voltage deviation predefined value under SM malfunction", *International Journal of Electrical Power & Energy Systems*, 156, 109729, 2024. <https://doi.org/10.1016/j.ijepes.2023.109729>.

[15]Guo, L., Sun, Y., & Jin, N, "A Capacitor Voltage Balancing Control Strategy for Modular Multilevel Converter", *Electric Power Components and Systems*, 48(12–13), 1410–1420,2020. <https://doi.org/10.1080/15325008.2020.1856230>.

[16]Konstantinou, G., Wickramasinghe, H. R., Townsend, C. D., Ceballos, S., & Pou, J, " Estimation Methods and Sensor Reduction in Modular Multilevel Converters", A Review. 2018 8th International Conference on Power and Energy Systems (ICPES), 23–28,2018. <https://doi.org/10.1109/ICPESYS.2018.8626987>.

[17]Abushafa, O. S. H. M., Dahidah, M. S. A., Gadoue, S. M., & Atkinson, D. J, "Submodule Voltage Estimation Scheme in Modular Multilevel Converters with Reduced Voltage Sensors Based on Kalman Filter Approach", *IEEE Transactions on Industrial Electronics*, 65(9), 7025–7035,2018. <https://doi.org/10.1109/TIE.2018.2795519>.

[18]Islam, M. D., Razzaghi, R., & Bahrani, B, "Arm-Sensorless Sub-Module Voltage Estimation and Balancing of Modular Multilevel Converters", *IEEE Transactions on Power Delivery*, 35(2), 957–967,2020. <https://doi.org/10.1109/TPWRD.2019.2931287>.

[19]Liu, H., Ma, K., Loh, P. C., & Blaabjerg, F, " A sensorless control method for capacitor voltage balance and circulating current suppression of modular multilevel converter", 2015 IEEE Energy Conversion Congress and Exposition (ECCE), 6376–6384,2015. <https://doi.org/10.1109/ECCE.2015.7310553>.

[20]Abdelsalam, M., Marei, M., Tennakoon, S., & Griffiths, A, "Capacitor voltage balancing strategy based on sub-module capacitor voltage estimation for modular multilevel converters", *CSEE Journal of Power and Energy Systems*, 2(1), 65–73, 2016. <https://doi.org/10.17775/CSEEJPES.2016.00010>.

[21]Trabelsi, M., Ghanes, M., Ellabban, O., Abu-Rub, H., & Ben-Brahim, L, "An interconnected observer for modular multilevel converter", 2016 IEEE Energy Conversion Congress and Exposition (ECCE), 1–7. 2016. <https://doi.org/10.1109/ECCE.2016.7854853>.

[22]da Silva, G. S., Vieira, R. P., & Rech, C, "Modified sliding-mode observer of capacitor voltages in Modular Multilevel Converter", 2015 IEEE 13th Brazilian Power Electronics Conference and 1st Southern Power Electronics Conference (COBEP/SPEC), 1–6, 2015). <https://doi.org/10.1109/COBEP.2015.7420217>.

- [23] Luo, Y., Wang, F., Bai, T., Guo, H., & Feng, X, "A Sensorless Control Method for MMC Based on Sliding Mode Observer", 2018 IEEE International Power Electronics and Application Conference and Exposition (PEAC), 1–6, 2018. <https://doi.org/10.1109/PEAC.2018.8590231>.
- [24] da Silva, G. S., Vieira, R. P., & Rech, C, "Discrete-Time Sliding-Mode Observer for Capacitor Voltage Control in Modular Multilevel Converters", IEEE Transactions on Industrial Electronics, 65(1), 876–886, 2018. <https://doi.org/10.1109/TIE.2017.2721881>.
- [25] Hafez, A. A., Mahmoud, A. A., & Yousef, A. M, "Robust and Intelligent Control for Single-stage Grid-Connected Modular Multilevel Converter in PV Applications", Journal of Electrical Engineering & Technology, 16(2), 917–931, 2021. <https://doi.org/10.1007/s42835-020-00639-8>.
- [26] Imane, A., Imad, M., & Osama, A, "Robust and Intelligent Control for PV System of Two Converters: DC-DC Converter/ Single-Phase Modular Multilevel Converter to Operate Grid Connected", 2023 International Conference on Decision Aid Sciences and Applications (DASA), 278–283, 2023. <https://doi.org/10.1109/DASA59624.2023.10286773>.
- [27] Guo, L., Li, Y., Jin, N., Dou, Z., & Wu, J, "Sliding mode observer-based AC voltage sensorless model predictive control for grid-connected inverters", IET Power Electronics, 13(10), 2077–2085, 2020. <https://doi.org/10.1049/iet-pel.2019.1075>.
- [28] Guo, B., Su, M., Wang, H., Tang, Z., Liao, Y., Zhang, L., & Shi, S, "Observer-based second-order sliding mode control for grid-connected VSI with LCL-type filter under weak grid", Electric Power Systems Research, 183, 106270, 2020. <https://doi.org/10.1016/j.epsr.2020.106270>.
- [29] Mahmoud, A. A., Hafez, A. A., Yousef, A. M., Gaafar, M. A., Orabi, M., & Ali, A. F. M, "Fault-tolerant modular multilevel converter for a seamless transition between stand-alone and grid-connected microgrid", IET Power Electronics, 16(1), 11–25, 2023. <https://doi.org/10.1049/iet-pel.2023.12359>.
- [30] Hagiwara, M., & Akagi, H, "Control and Experiment of Pulsewidth-Modulated Modular Multilevel Converters", IEEE Transactions on Power Electronics, 24(7), 1737–1746, 2009. <https://doi.org/10.1109/TPEL.2009.2014236>.
- [31] Nguyen, V.-T., Kim, J.-W., Lee, J.-W., & Park, B.-G, "Optimal Design of a Submodule Capacitor in a Modular Multilevel Converter for Medium Voltage Motor Drives", Energies, 17(2), 471, 2024. <https://doi.org/10.3390/en17020471>.
- [32] Lyu, Y., Zi, Y., & Li, X, "Improved Control of Capacitor Voltage Balancing in Modular Multilevel Converter Submodules", IEEE Access, 12, 19510–19519, 2024. <https://doi.org/10.1109/ACCESS.2024.3350178>.
- [33] Nguyen, M. H., Kwak, S., & Kim, T, "Phase-Shifted Carrier Pulse-Width Modulation Algorithm With Improved Dynamic Performance for Modular Multilevel Converters", IEEE Access, 7, 170949–170960, 2019. <https://doi.org/10.1109/ACCESS.2019.2955714>.
- [34] Luo, D., Lin, D., Zhang, W., & Lian, W, "A novel jittered-carrier phase-shifted sine pulse width modulation for cascaded H-bridge converter", The Journal of Engineering, 2024(6), 2024. <https://doi.org/10.1049/tje2.12391>.